Mycorrhiza (1999) 9:205–213

ORIGINAL PAPER

Sandy Dickson · Peter Kolesik

Visualisation of mycorrhizal fungal structures and quantification of their surface area and volume using laser scanning confocal microscopy

Accepted: 25 August 1999

Abstract A method has been developed for the visualisation and three-dimensional (3D) measurement of mycorrhizal fungal structures inside plant roots. Sections of *Allium porrum* L. roots colonised by *Glomus* sp. 'City Beach' (WUM 16) and *Lilium* sp. roots colonised by *Scutellospora calospora* (Nicol. & Gerd.) Walker & Sanders (WUM 12(2)) were stained with acid fuchsin. This allowed fluorescence from the fungal structures to be observed under a laser scanning confocal microscope (LSCM) without interference from the plant cells. A series of horizontal optical sections were collected from a *Glomus* sp. arbuscule and from a hyphal coil of *S. calospora*. These data were used to produce extended focus images. Axial distortion in microscopic visualisation due to the refractive index mismatch between the immersion and mounting media was quantified using vertical scanning of the hyphae. A correction factor of 0.71 μm was used for the z-interval between the xy-slices. A series of binary xy-images from each structure was rendered into a 3D graphical model for viewing. The volume and surface area of the structures were estimated using computerised 3D measurement and also by stereological integration of binary xy-images. With both structures, the surface area estimates varied greatly between the two measuring systems, whereas differences in volume estimates were small. Computerised 3D measurement was considered more accurate than stereological integration of confocal binary images.

Key words Arbuscular mycorrhiza · Staining · Visualisation · Confocal microscopy · Quantification

S. Dickson (✉)
Department of Soil and Water and the Centre for Plant Root Symbioses,
The University of Adelaide,
Waite Campus, PMB 1,
Glen Osmond, South Australia 5064, Australia
e-mail: sdickson@waite.adelaide.edu.au
Tel.: +61-8-83036530, Fax: +61-8-83036511

P. Kolesik
Department of Horticulture,
Viticulture and Oenology and the Centre for Plant Root Symbioses,
The University of Adelaide,
Waite Campus, PMB 1,
Glen Osmond, South Australia 5064, Australia

Introduction

Over 80% of terrestrial plants are able to associate symbiotically with mycorrhizal fungi and this usually results in a positive plant growth response (Smith and Read 1997). Mutual nutrient transfer between the fungus and the plant provides the plant with phosphate and micronutrients such as copper and zinc and the fungus with carbon-based compounds. The most common form of symbiosis involves arbuscular mycorrhizal (AM) fungi, which form two major structural classes of mycorrhiza with different host plants: *Arum*- and *Paris*-types (Gallaud 1905). *Arum*-type colonisation includes intercellular hyphae, arbuscules and sometimes vesicles, while *Paris*-type colonisation has intracellular hyphal coils with intercalary arbuscules in cortical cells and, again, sometimes vesicles (Smith and Smith 1997). The type of mycorrhiza formed depends on the host plant and a single fungus can form either type (e.g. Barrett 1958; Brundrett and Kendrick 1990).

In AM fungi, arbuscules are considered the major site of nutrient transfer to the plant (Cox and Sanders 1974; Smith and Smith 1990). In plants forming *Paris*-type mycorrhiza, although arbuscules may be present in the fungal life cycle, intracellular coils appear to form a large proportion of the fungal mass within the plant cells. The functional relevance of the coils, in terms of the area of interface capable of nutrient transfer, has yet to be determined (Smith and Smith 1996). The efficiency of phosphate transfer from fungus to plant (or carbon in the reverse direction) can be expressed as fluxes across the plant-fungus symbiotic interface. This requires estimates of the interface surface area.

Traditional methods of estimating volume and surface area of arbuscules use morphometric techniques based on a number of electron micrographs (Cox and Tinker 1976; Toth and Miller 1984; Alexander et al. 1988, 1989). Cox and Tinker (1976) took electron micrographs of eight arbuscules from onion (*Allium cepa*) root sections colonised by *Glomus mosseae*, measured them using image analysis and calculated the area and perimeter of the arbuscule in 2D. They calculated the invaginated plasmalemma of the arbuscule to be 2.07 times larger than the cell perimeter. Using a stereological equation derived by Underwood (1969), based on planar sections, to calculate the volume of a 3D structure, Cox and Tinker (1976) then calculated the phosophate flux across the symbiotic interface. Image analysis was also used by Smith and Dickson (1991) and Smith et al. (1994) to measure the perimeters of metabolically active arbuscules in cross-sections using bright field microscopy. The surface area of the structures was calculated using the value obtained by Cox and Tinker (1976) together with a correction factor for immature arbuscules. All of the above approaches are prone to considerable errors due to artefacts created by tissue preparation or by low precision of the measurement.

Laser scanning confocal microscopy (LSCM) allows fluorescently stained structures to be visualised with high resolution in fixed or fresh tissue by optical sectioning without the need for mechanical thin sectioning (Czymmek et al. 1994). Confocal visualisation of optical slices through structures in fresh material is free of possible changes in volume and surface area caused by fixation and embedding prior to sectioning. A series of optical slices through entire fungal structures allows 3D reconstructions to be created and quantitative estimates of surface area and volume to be obtained much more easily than with previous methods (König et al. 1991).

Various fluorochromes have been used to study fungal cytology and differentiation with fluorescence microscopy (Butt et al. 1989). An important requirement for the imaging and measurement of mycorrhizal fungal structures is that the stain discriminates between fungus and plant (Dickson and Smith 1998). Root segments stained with acid fuchsin and observed by fluorescence microscopy were used to determine the resolution of mycorrhizal structures (Merryweather and Fitter 1991). In the large number of plant species tested, fungal structures were clearly visible at low levels of colonisation but structures were obscured in heavily colonised roots. Melville et al. (1998) visualised mycorrhizal structures in several plant species using a range of xanthene dyes to determine the best staining technique for embedded material in the confocal system. However, these stains did not work well with fresh material. Fungal autofluorescence has been used recently for visualising *G. mosseae* in living roots of *Lolium perenne*. However, only collapsed arbuscules were observed and the intercellular hyphae did not autofluoresce very strongly (Vierheilig et al. 1999).

In this paper, we describe a method for freeze-sectioning and staining of fresh plant material for AM structures. LSCM was used to produce 2D and 3D images of arbuscules and a hyphal coil. Different levels of light intensity were used in the collecting of the images and the quality of the visualisation of the structures are shown. We compared surface area and volume estimates of the structures obtained using two binary image analysis approaches: true 3D rendering and stereological integration.

Materials and methods

Plant material and tissue preparation

Plants of *A. porrum* L. and *Lilium* sp. were inoculated with the AM fungi *Glomus* sp. 'City Beach' (WUM 16) and *Scutellospora calospora* (Nicol. & Gerd.) Walker & Sanders (WUM 12(2)), respectively. Plants were grown in a growth room with a 14-h photoperiod and temperatures of 23 °C and 18 °C light/dark phases. Photon flux density was 500 μmol m^{-2} s^{-1}. Plants were harvested and roots washed free of soil. Root material was cut into approximately 1-cm lengths and embedded into gelatin blocks containing 10% (w/v) gelatine and 2% glycerol. Blocks were frozen on a Microm K-400 freezing stage and 120-μm-thick longitudinal sections were cut using a Leitz 1320 freezing microtome following a modified method of Smith and Dickson (1991).

Staining of fresh material

Sections, prepared as above, were stained overnight in a solution containing lactic acid, glycerol, distilled water and 0.01% acid fuchsin (Brundrett et al. 1994). Sections were removed from gelatin by rinsing with warm water, mounted in 100% glycerol between glass spacers on glass slides, covered with a cover slip and sealed with nail polish. Samples were screened by epifluorescence microscopy using a Zeiss Standard Lab 16 microscope and filter set with excitation of 450–530 nm and emission of 455–490 nm. Sites of interest (containing coils or arbuscules) were marked on the slides for subsequent visualisation by LSCM.

Sulphorhodamine G and phloxine B were also tested for differential staining of the fungi within fresh roots (Canny and McCully 1986; Melville et al. 1998), but neither fluoresced strongly using the following three combinations of fluorescent filters: excitation (ex) 488/10 nm & emission (em) 522/35 nm, ex 568/10 nm and em 605/35 nm or ex 647/10 nm and em 680/32 nm.

Confocal visualisation

Microscopy

A Bio-Rad MRC-1000 laser scanning confocal microscope system in combination with a Kr/Ar laser and a Nikon Diaphot 300 inverted microscope in fluorescence mode with excitation at 488/10 nm and emission at 522/32 nm was used to visualise acid fuchsin staining. Samples were observed with a $\times 40$ water-immersion objective lens with a numerical aperture of 1.15 and working distance of 210 μm. A series of optical xy-slices, each with a 1-μm interval on the z-axis, was collected for both mycorrhizal structures. Each image was averaged over 8 scans using a Kalman filtering process and saved as a digital file with the size of 768×512 pixels; the intensity of staining was expressed in 256 levels of grey (0 = black, 255 = white).

Correction of axial distortion

The refractive index mismatch between the immersion medium of the objective lens (water, $RI = 1.33$), the combination of the embedding medium (glycerol, $RI = 1.47$) and the plant and fungal tissue (RI unknown) resulted in over-estimation of the actual depth of tissue visualised by LSCM. Correction of the nominal z-distance between the optical slices was required (White et al. 1996). X- and y-diameters of hyphae oriented perpendicular to the visualised confocal xy-plane were measured for roundness. X- and z-diameters of hyphae oriented parallel to the y- and perpendicular to the z-axis were measured on optical yz-slices collected by vertical scanning to evaluate the extent of optical stretching along the z-axis. A correction factor for axial distortion was calculated using the ratio of x- to z-diameter of the hyphae visualised vertically. For both mycorrhizal structures, electronic zoom was used during the image-collection process so that each optical slice was taken in the central, relatively planar focal plane of the objective lens.

Measurement of surface area and volume

Binary images of optical slices

Acid fuchsin bound predominantly to the cell walls and to a lesser extent to the cell interiors of the fungi. The coil image, recorded using a high intensity of laser, had optical slices that were oversaturated so that the interior of the hypha was also visible. This procedure allowed the complete structure to be discriminated in each optical slice. Arbuscules showed varying levels of fluorescent staining depending upon the size of the hyphal branches (Fig. 1). First-order branches of the arbuscules appeared undersaturated while 3rd-order branches were slightly oversaturated. An intensity threshold separating hyphae from the background was used (Fig. 2a) to create binary masks for the whole z-series of the arbuscule. Due to the varying intensities of staining in the interiors of the 2nd- and 3rd-order branches, the hyphal interiors were manually filled in to produce a complete image of the structure in each binary slice using Scion Image software (Fig. 2b). These 2D binary masks of z-optical sections were then rendered into a 3D model of the fungal structure.

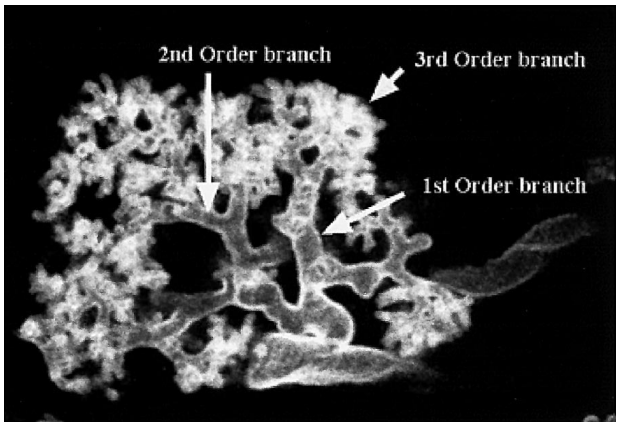

Fig. 1 Integration of several optical sections through an arbuscule showing the differences in fluorescent staining due to the diameter of the hyphal branches

3D reconstruction

The binary masks of the z-series, expressed in pixels, were rendered into a 3D isointensity contoured object, expressed in voxels, by the marching cubes algorithm using ImageVolumes 2·0 (Minnesota Datametrics Corporation, USA) software and a Silicon Graphics Indigo 2 computer. The 3D model was visualised and its volume and surface area measured.

Stereology

The individual binary masks were also measured using the Video Pro 32 Colour Image Analysis System (Leading Edge Pty Ltd, Australia). The area and perimeter of the central arbuscule were measured in each optical slice in the z-series and the total area and perimeter determined. The volume and surface area of an entire fungal structure in 3D were calculated as the arithmetical product of the total area and perimeter, respectively, and the z-distance between the optical slices.

Results

Staining

Of the three stains examined, only acid fuchsin performed satisfactorily. Light pink staining of the fungus produced a fluorescent signal clearly visible under the confocal system with nearly no signal coming from the plant cells. Staining, however, was irregular due to the uneven thickness of the arbuscular branches. Trunk hyphae (1st-order branches) were relatively thick (3.02 ± 0.06 μm diameter, $n = 20$) (mean ± SD) and the fluorescent signal appeared weak inside the hyphae (see Fig. 1). Branches of the 2nd-order (1.64 ± 0.07 μm diameter, $n = 20$) were also stained unevenly but fluorescence was clearly detectable inside the hyphae. The smallest branches (1.08 ± 0.06 μm diameter, $n = 20$) generally fluoresced strongly with a partial oversaturation of the signal.

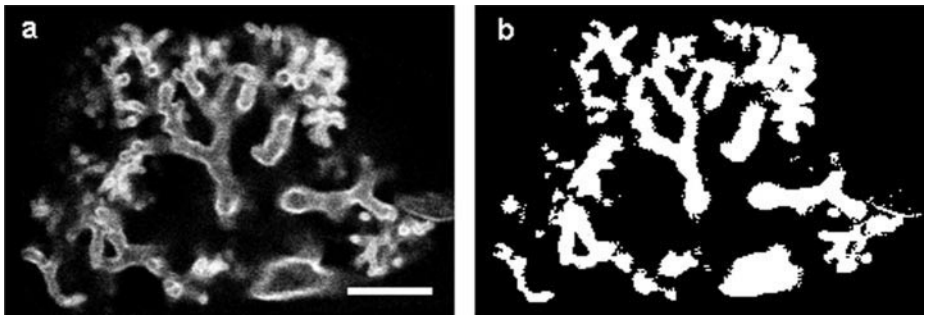

Fig. 2 A single optical section through an arbuscule showing (**a**) the intensity of the fluorescent signal and (**b**) the binary mask created using a determined threshold level and filling in non-discriminated interiors; *bar* 10 μm

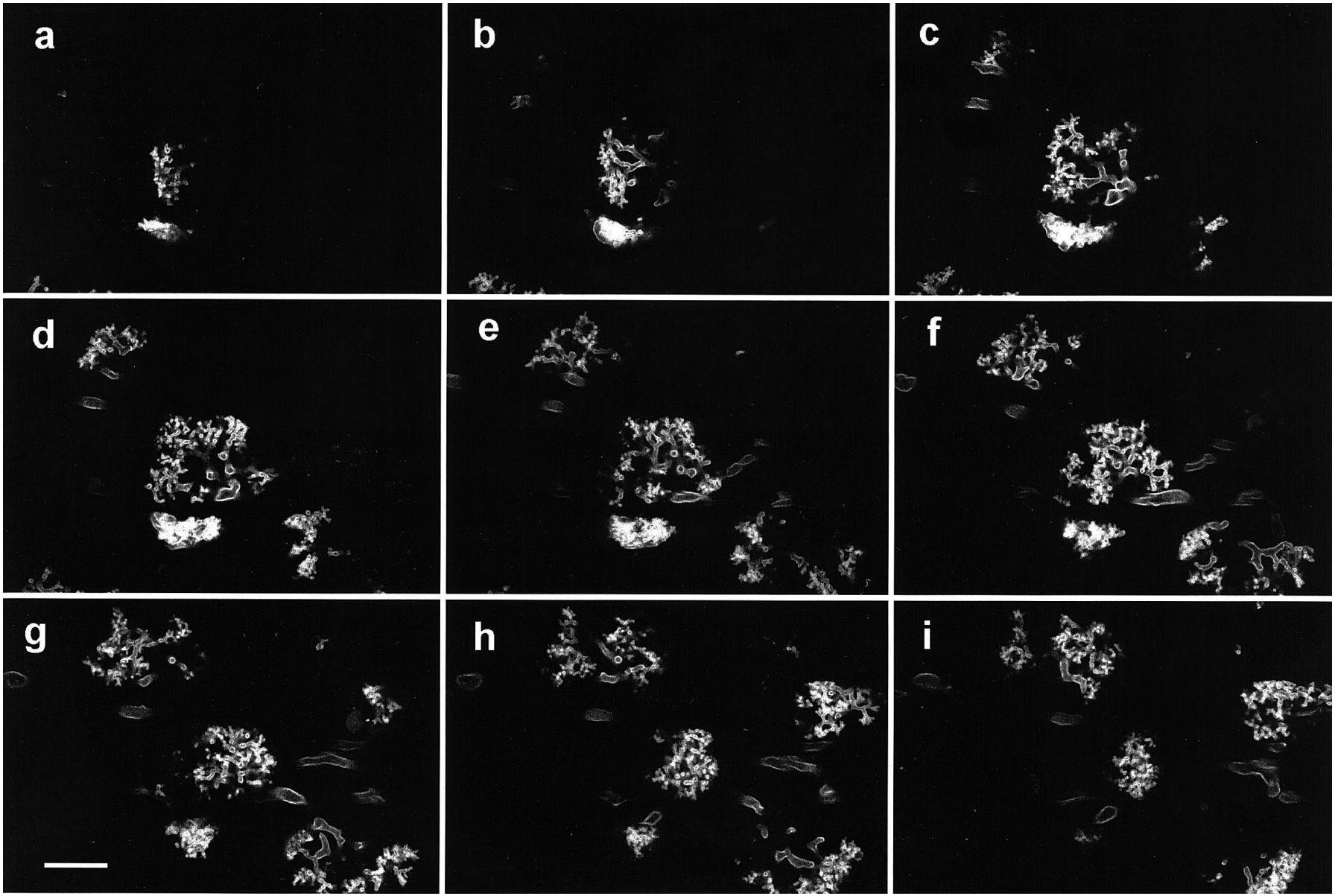

Fig. 3a–i Representative optical slices through a group of *Arum*-type arbuscules of *Glomus* sp. 'City Beach' in *Allium porrum* shown at 2.1 intervals on the z-axis; *bar* 25 μm

Confocal microscopy

Visualisation

Forty-one xy-images were taken along the z-axis of a group of *Glomus* sp. 'City Beach' *Arum*-type arbuscules in *A. porrum* cortical root cells. Representative optical slices are shown in Fig. 3a–i at 2.1-μm intervals on the z-axis (corrected z-distance). These images were recorded with an unsaturated intensity of fluorescent signal in order to produce a visually acceptable extended focus image. The difference in brightness of the various orders of hyphal branching is clearly noticeable in the individual slices. An extended focus image of the arbuscules (11 images merged at 2.1-μm intervals) is shown in Fig. 4. The x-dimension of the central arbuscule (boxed) was 49 μm, y-dimension 54 μm and z-dimension 22 μm.

Representative xy-images from a total of 39 images of a *Paris*-type coil in a *Lilium* sp. cortical root cell are shown in Fig. 5a–i. The selected optical slices were at 2.1-μm intervals on the z-axis (corrected z-distance). Parts of the images appeared bright and were slightly oversaturated in the individual optical slices. The extended focus image of the hyphal coil (13 images merged at 2.1-μm intervals) is shown in Fig. 6. Combining these slices to form an extended focus image was less satisfactory in quality than the composite image formed of the arbuscule because definition within the coil structure was lost. The x-dimension of this hyphal coil was 48 μm, y-dimension 33 μm and z-dimension 28 μm.

Correction of axial distortion

The mean ratio between the x- and y-diameters of the hyphae visualised by horizontal scanning demonstrated that hyphae were round in cross-section (1.00 ± 0.01 SD, $n = 10$) and, therefore, could be considered as cylindrical. The mean ratio between the x- and z-diameters was 1.40 ± 0.11 SD ($n = 10$), which indicated a 1.40 times stretch of the optical signal along the z-axis. Based on this axial distortion the nominal z-interval between the xy-slices of 1.0 μm was corrected to 0.71 μm.

3-D reconstruction

The binary masks of the central arbuscule were set at the threshold of 95 for all 31 optical slices and 207 for all 39 optical slices of the coil. 3D image reconstruction, created from the binary masks of the central arbuscule in Fig. 4, is shown in Fig. 7. The 3D image looks similar to the result produced by the extended focus image showing detail of the hyphal branches (Fig. 3). The coil (Fig. 8), which was recorded as an oversaturated confocal image, is clearly defined in 3D.

Measurement of surface area and volume

Table 1 shows the estimates of surface area and volume of the two fungal structures using 3D rendering (ImageVolumes) and stereological integration (Video Pro). With both structures, the surface area estimates varied greatly between the two measuring systems, whereas differences in volume estimates were small. Video Pro

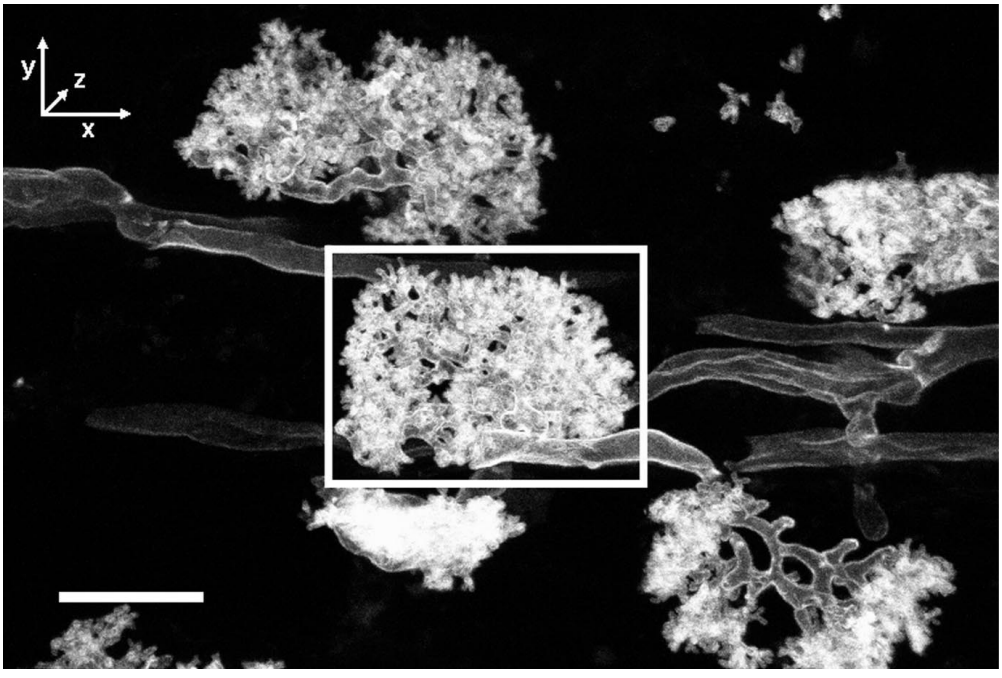

Fig. 4 An extended focus image of a group of *Arum*-type arbuscules of *Glomus* sp. 'City Beach' in *A. porrum* (11 images merged at 2.1 intervals); *bar* 25 μm

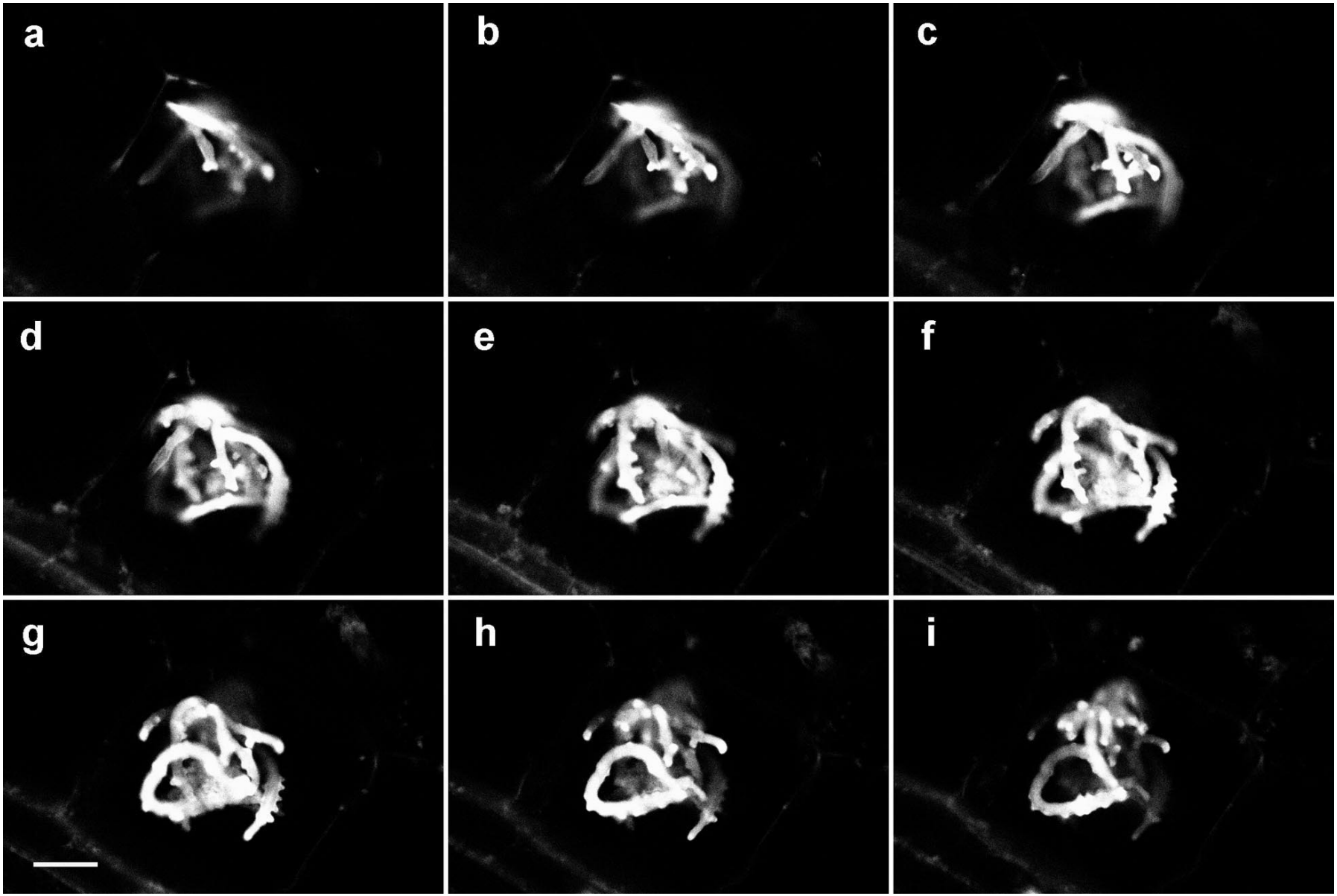

Fig. 5a–i Representative optical slices through a *Paris*-type coil of *Scutellospora calospora* in *Lilium* sp. shown at 2.1 intervals on the z-axis; *bar* 25 μm

produced much smaller estimates for surface area than ImageVolumes. This led to substantial differences in the surface area/volume ratios for both structures. Both methods of measuring the arbuscule produced much greater ratios than those obtained for the coil.

Discussion

Only fungal material that appeared very lightly stained was brightly fluorescent under the confocal system. This situation precluded visual assessment of the extent of mycorrhizal colonisation using conventional bright field light microscopy in sectioned roots. When time of acid fuchsin staining was lengthened or the staining repeated to make fungal tissue easily observable with light microscopy, fluorescence was quenched to a suboptimal level. Weak fluorescence of strong acid fuchsin staining could be partly remedied by uncaging the dye into a strong fluorescence response by exposing the section to a higher intensity laser beam before imaging. However, this treatment extended the time for sample visualisation considerably and also increased the background signal. Alternatively, the use of the red laser line (ex 647 nm) allowed confocal visualisation of the fungi in samples optimally stained for bright field microscopy. However, the plant cells could also be visualised and extensive background signal was present. Using the combination of the 647 nm laser line and acid fuchsin staining does not seem practical for 3D reconstruction and measurements of fungal attributes, although it may be useful in the calculation of plant cell volume in relation to that of the fungal structure inside.

There are two different purposes for image processing: 1) to improve the visual appearance of images to the human viewer and 2) to prepare images for measurement of features and structures. It is not possible to manipulate the data enough once it has been collected by LSCM to perform both functions of observation and measurement. The aim of any experiment must, therefore, be clearly defined before data collection is performed.

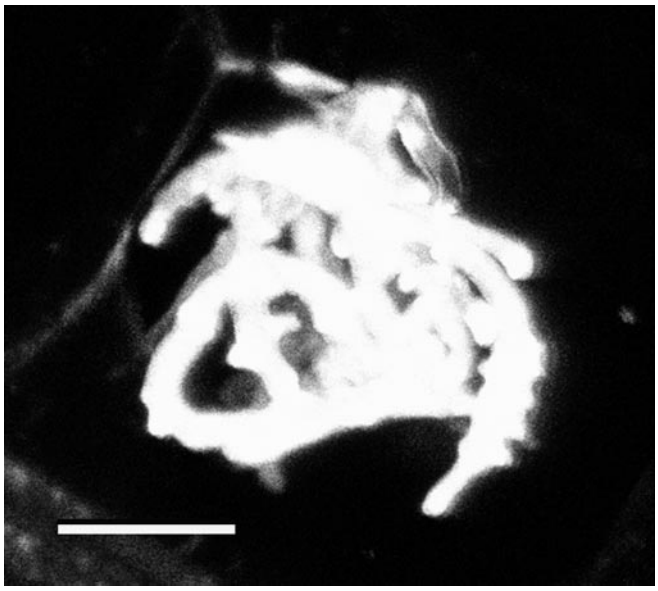

Fig. 6 An extended focus image of a *Paris*-type coil of *S. calospora* in *Lilium* sp.(13 images merged at 2.1 intervals); *bar* 25 μm

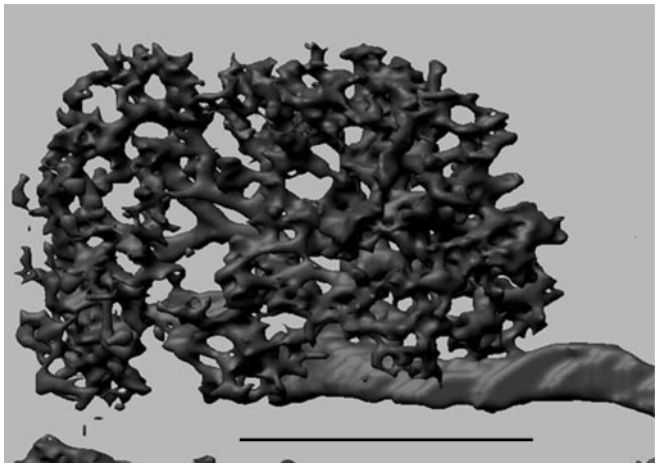

Fig. 7 3D reconstruction of an arbuscule of *Glomus* sp. 'City Beach' in *A. porrum* from within the group shown in Fig. 4; *bar* 25 μm

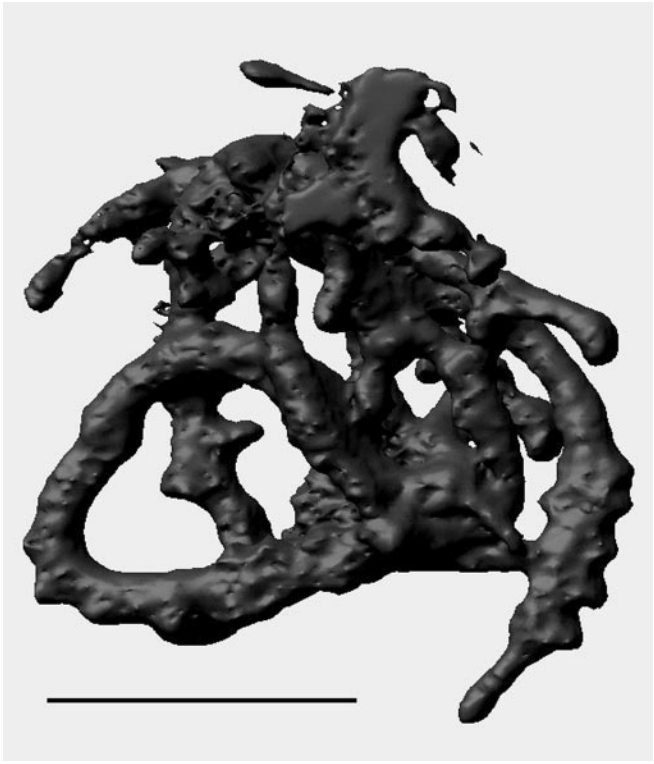

Fig. 8 3D reconstruction of the hyphal coil of *S. calospora* in *Lilium* sp. shown in Fig. 5; *bar* 25 μm

Table 1 Estimates of surface area and volume of arbuscule and coil using 3D rendering (ImageVolumes 2.0) and stereological integration (Video Pro 32 Colour Image Analysis System)

		Image Volumes	Video Pro
Arbuscule	Surface area (μm^2) (SA)	8672	6595
	Volume (μm^3)(V)	3375	3171
	SA/V ratio (μm^{-1})	2.57	2.08
Coil	Surface area (μm^2) (SA)	12552	8439
	Volume (μm^3) (V)	13783	13586
	SA/V ratio (μm^{-1})	0.91	0.62

There are both advantages and disadvantages of recording unsaturated images. Optimally stained samples sometimes photobleached slightly during collection of the data and, consequently, the signal-to-noise ratio was decreased. In these cases, a sliding threshold is required to compensate for differences in signal intensity through the optical sections. As shown in Figs. 3 and 4 (arbuscules), individual optical slices and composite images collected from optimally unsaturated material have a high resolution. The 3D reconstruction of the central structure shows the detail of many of the branches, although it does not exactly reproduce the extended focus image (Fig. 7). In a finely detailed structure such as this, depending upon the thresholding, an underestimation of surface areas and overestimation of volumes are possible. On the other hand, oversaturated images (Figs. 5, 6, 8 - coil) provide us with possibly more complete measurements from the 3D reconstruction, but the extended focus image shows less definition.

Measurements of both the arbuscule and the coil using 3D rendering (ImageVolumes) and stereology (Video Pro) produced similar estimates for volume but not for surface area (Table 1). The arbuscule had a much larger surface area in relation to volume. Coil branches were much wider (5.56 ± 1.22 μm, $n = 32$) and less numerous than the arbuscular branches (see Figs. 7, 8), leading to the coil having a greater volume in relation to surface area than the arbuscule using both measuring methods. Surface areas determined by Video Pro were much smaller than those obtained using ImageVolumes due to the nature of the software programmes.

The measurements obtained by 3D rendering using ImageVolumes are more accurate than those calculated by a simple stereological integration using Video Pro. The mode of integrating the 2D binary masks using the two approaches differ. 3D rendering used a polygon and voxel generator to process serial section data and stored it as a 3D geometric database of surface polygons and voxel densities. These data were smoothed using a 2×2 median filter and were rendered into a 3D structure which was then measured. Stereological integration combined the measurements of individual optical slices using a 3×3 median filter into a total surface area and volume which were then multiplied by the z-distance. Mathematical integration did not take into account the relative position of the optical slices to each other. While integration had little effect on the total volume of the structures, the surface area estimates were underestimated to a much greater degree than can be accounted for by the use of the 3×3 median filter. The value of this underestimation will depend upon the size and complexity of the structure involved. Using stereology, the estimate of the surface area of the coil was underestimated to a greater extent than for the arbuscule.

Previously, stereological methods have been used to measure arbuscules by measuring the surface area of the structure in relation to the cell volume using the equation $S_V = 4N_L$ where S_V is the surface area per unit volume and N_L is the number of times the test lines intercept the host plasmalemma (Toth 1982; Alexander et al. 1988, 1989). This equation does not determine the surface area of the structure in relation to its own volume but to the test volume, such as that of the cell containing the arbuscule (Toth 1992). Calculation of the surface area using volume fractions can be difficult because of shrinkage due to resin embedding. The magnification of the final micrographs also needs to be optimised for measuring with a superimposed grid pattern. Alexander et al. (1989) measured arbuscules in onion (*Allium cepa*), bean (*Phaseolus vulgaris*) and tomato (*Lycopersicon esculentum*) and obtained an average volume of 32 963 μm^3. This value is much larger than the values we obtained (3 171–3 375 μm^3 using our two methods). Although Alexander et al. (1988, 1989) quantified a large number of arbuscules in various stages of development and degeneration in their experiments, all parameters measured were compared to that of a mature arbuscule. If a cell when randomly cut went through a highly developed arbuscule but appeared to be from a 'young developing-looking' arbuscule then volume data would be overestimated (Toth 1992). Our arbuscule may not have been as fully developed or highly branched as those examined by Alexander et al. (1989). They also used different fungal species (*G. fasciculatum*) and plant, which may account for some of the differences. We realise that further measurements are required, using a range of arbuscules of various ages and from different plant and fungal species, in order to make a more valid comparison. These measurements may then be used to compare the size of arbuscules formed and to calculate the rates of transfer across interfaces between the mycorrhizal symbionts.

In conclusion, our study shows that acid fuchsin can be used for the staining of fungal structures in fresh plant roots for visualisation using LSCM. The confocal 3D rendering method of volume and surface area meas-

urements presented is applicable to a range of mycological morphometric analyses. It provides measurement estimates much more easily and quickly than previously attainable, particularly for complex structures, and does not suffer from the problems of other morphometric techniques, such as resin embedding and stereological integration. Given adequate computer software, this technique allows a large number of measurements to be obtained for fungal comparison and nutrient transfer calculations. Furthermore, the technique is likely to prove useful for the study of associations of plant pathogenic fungi with host tissues.

Acknowledgements We wish to thank S.E. Smith, F.A. Smith, A.R. Humpage and S.M. Ayling for helpful comments and I.J. Gibbins of The Flinders University of South Australia for access to ImageVolumes. S. D. is funded by an Australian Research Council grant-funded scholarship.

References

Alexander T, Meier R, Toth R, Weber HC (1988) Dynamics of arbuscule development and degeneration in mycorrhizas of *Triticum aestivum* L. and *Avena sativa* L. with reference to *Zea mays* L. New Phytol 110:363–370

Alexander T, Toth R, Meier R, Weber HC (1989) Dynamics of arbuscule development and degeneration in onion, bean and tomato with reference to vesicular-arbuscular mycorrhizae with grasses. Can J Bot 67:2505–2513

Barrett JT (1958) Synthesis of mycorrhiza with pure cultures of *Rhizophagus*. Phytopathology 48:391

Brundrett M, Kendrick B (1990) The roots and mycorrhizas of herbaceous woodland plants. II. Structural aspects of morphology. New Phytol 114:469–479

Brundrett M, Melville L, Peterson RL (eds) (1994) Practical methods in mycorrhizal research. Mycologue, Waterloo, Canada

Butt TM, Hoch HC, Staples RC, St Leger RJ (1989) Use of fluorochromes in the study of fungal cytology and differentiation. Exp Mycol 13:303–320

Canny MJ, McGully ME (1986) Locating water-soluble vital stains in plant tissue by freeze- sectioning and resin embedding. J Microsc 142:63–70

Cox G, Sanders F (1974) Ultrastructure of the host-fungus interface in a vesicular-arbuscular mycorrhiza. New Phytol 73:901–912

Cox G, Tinker PB (1976) Translocation and transfer of nutrients in vesicular-arbuscular mycorrhizas. I. The arbuscule and phosphorus transfer: a quantitative ultrastructural study. New Phytol 77:371–378

Czymmek KJ, Whallon JH, Klomparens KL (1994) Confocal microscopy in mycological research. Exp Mycol 18:275–293

Dickson S, Smith SE (1998) Evaluation of vesicular-arbuscular mycorrhizal colonisation by staining. In: Varma A (ed) Mycorrhiza manual. Springer, Berlin Heidelberg, pp 77–83

Gallaud I (1905) Etudes sur les mycorrhizes endotrophs. Rev Gen Bot 17:5–48, 66–83, 123–135, 223–239, 313–325, 425–433, 479–500

König D, Carvajal Gonzalez S, Downs AM, Vassey J, Rigaut JP (1991) Modelling and analysis of 3-D arrangements of particles by point processes with examples of application to biological data obtained by confocal scanning light microscopy. J Microsc 161:405–433

Melville L, Dickson S, Farquhar ML, Smith S, Peterson RL (1998) Visualization of mycorrhizal fungal structures in resin embedded tissues with xanthene dyes using laser scanning confocal microscopy. Can J Bot 76:174–178

Merryweather JW, Fitter AH (1991) A modified method for elucidating the structure of the fungal partner in a vesicular-arbuscular mycorrhiza. Mycol Res 95:1435–1437

Smith FA, Smith SE (1997) Structural diversity in (vesicular)-arbuscular mycorrhizal symbiosis. New Phytol 137:373–388

Smith SE, Dickson S (1991) Quantification of active vesicular-arbuscular mycorrhizal infection using image analysis and other techniques. Aust J Plant Physiol 18:637–648

Smith SE, Read DJ (1997) Mycorrhizal symbiosis, 2nd edn. Academic, Cambridge, UK

Smith SE, Smith FA (1990) Structure and function of the interfaces in biotrophic symbioses as they relate to nutrient transport. New Phytol 114:1–38

Smith SE, Smith FA (1996) Membranes in mycorrhizal interfaces: specialised functions in symbiosis. In: Smallwood M, Knox JP, Bowles D (eds) Membranes: specialised functions in plant cells. Bios, Oxford, UK, pp 525–542

Smith SE, Dickson S, Morris C, Smith FA (1994) Transport of phosphate from fungus to plant in VA mycorrhizas: calculation of the area of symbiotic interface and of fluxes from two different fungi to *Allium porrum* L. New Phytol 127:93–97

Toth R (1982) An introduction to morphometric cytology and its application to botanical research. Am J Bot 69:1694–1706

Toth R (1992) Quantification of arbuscules and related structures using morphometric cytology. Methods Microbiol 24:275–299

Toth R, Miller RM (1984) Dynamics of arbuscule development and degeneration in a *Zea mays* mycorrhiza. Am J Bot 71:449–460

Underwood EE (1969) Stereology, or the quantitative evaluation of microstructures. J Microsc 89:161–180

Vierheilig H, Böckenoff A, Knoblauch M, Juge C, van Bel AJE, Grundler F, Piché Y, Wyss U (1999) *In vivo* observations of the arbuscular mycorrhizal fungus *Glomus mosseae* in roots by confocal laser scanning microscopy. Mycol Res 103:311–314

White NS, Errington RJ, Fricker MD, Wood JL (1996) Aberration control in quantitative imaging of botanical specimens by multidimensional fluorescence microscopy. J Microsc 181:99–116